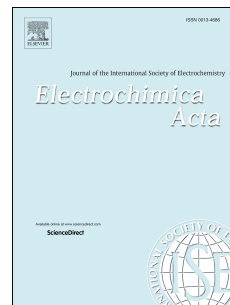# Accepted Manuscript

Optimization and characterization of nanostructured paper-based electrodes

A. Sánchez-Calvo, E. Núñez-Bajo, M.T. Fernández-Abedul, M.C. Blanco López, A. Costa García

Please cite this article as: A. Sánchez-Calvo, E. Núñez-Bajo, M.T. Fernández-Abedul, M.C. Blanco López, A. Costa García, Optimization and characterization of nanostructured paper-based electrodes, *Electrochimica Acta* (2018), doi: 10.1016/j.electacta.2018.01.179.

This is a PDF file of an unedited manuscript that has been accepted for publication. As a service to our customers we are providing this early version of the manuscript. The manuscript will undergo copyediting, typesetting, and review of the resulting proof before it is published in its final form. Please note that during the production process errors may be discovered which could affect the content, and all legal disclaimers that apply to the journal pertain.

1

OPTIMIZATION AND CHARACTERIZATION OF NANOSTRUCTURED PAPER-BASED ELECTRODES

4

A. Sánchez-Calvo, E. Núñez-Bajo, M.T. Fernández-Abedul, M.C. Blanco López[a], A. Costa García[b]

Departamento de Química Física y Analítica, Facultad de Química, Universidad de

Oviedo, 33006 Oviedo, Spain

a. **Corresponding author. cblanco@uniovi.es**
b. **Corresponding author. costa@uniovi.es**

13

14   **Abstract**.

15   Paper-based working electrodes were modified by the addition of nanomaterials (carbon

16   nanofibers, gold nanoparticles, graphene and hybrids of them), with the aim to increase

17   the conductivity and to obtain an electroactive platform with improved analytical

18   behaviour. The effect of the nanostructures was evaluated by using cyclic voltammetry

19   and dopamine as electrochemical probe. The modifications with *in-situ* generated

20   nanomaterials such as gold nanoparticles (AuNPs) or others requiring treatment like

21   graphene oxide (GO), were optimized by factorial design. The characterization of the

22   cellulose based electrodes by scanning electron microscopy (SEM) showed the

23   distribution of carbon nanofibers and the presence of AuNPs around the cellulose fibers.

24   The partial modification made by the carbon ink was also monitored by attenuated total

25   reflection (ATR) spectrometry. Electrodes modified with rGO and AuNPs exhibited

26   higher intensity peaks with more reversibility and reproducibility than unmodified

27   paper. The highest intensities and lowest limits of detection were achieved with paper

28   electrodes modified with hybrid nanostructures composed by both CNFs and AuNPs.

29

30   **Keywords.** Paper electrodes, carbon nanomaterials, gold nanoparticles, factorial design,

31   dopamine.

32

33

34

35

1. __Introduction__

One of the actual trends in sensor research is the development of low cost electrodes with low volume requirements, easy fabrication and simplicity, but without losing selectivity or reproducibility [1]. Among the materials that can be used as substrate for sensing devices, paper is a very attractive option [2-4]: it is mainly composed of a porous three-dimensional network of cellulose-fibres, which can transport either reagents or samples towards a detection chamber [5]. The electrochemical detection in Paper Analytical Devices (ePADs) has been recently reviewed [6]. These substrates can also be modified by the addition of hydrophobic materials such as wax, to form barriers, which define the biosensor area [7-9]. There is also a great variety of options on capillary flow rate and chemical adsorption, depending on the pore size and surface treatments applied. This allows choosing the best substrate for every target analyte. Besides, several types of paper with different pore size can be combined by origami strategies, to design the optimum sensor for biomarkers, heavy metal detection or the required application [10-17].

Modification of the cellulose network is usually necessary to develop a suitable electrochemical sensor, since cellulose is a non-conductive and porous material. However, some areas can be covered by conductive materials, to allow the study of electrochemical signals and optimize the performance of the electrodes [18-19]. There are several ways to modify the cellulose network to have a conductive surface, like gold sputtering or printing conductive inks, but the easiest way to achieve this conductive surface is drop casting an aliquot of carbon-ink suspension at the selected area. With this procedure, the modified paper can act as a working electrode, where the electrochemical reactions take place [20]. Paper-based working electrodes can also be modified by monolayers or electrogenerated polymers or nanomaterials such as gold

61 nanoparticles (AuNPs). An auxiliary and a reference electrode are then required to

62 construct the electrochemical cell, but these electrodes can also be printed with carbon

63 or other materials like silver [21]. There are also more options like connecting the

64 working paper electrode to screen-printed electrodes or external systems like gold-

65 plated pins [22]. This design with the screen-printed electrode placed below the paper

66 substrates has been applied in or group to the determination of arsenic in wines,

67 showing that it was possible to reuse the screen-printed electrode with another working

68 paper-based electrode without any interference. This resulted on a suitable and

69 sustainable route for sensor development [23].

70   In this paper, we have carried out for the first time a systematic study of the

71 optimization of the electrochemical properties of paper electrodes, modified by the

72 addition of several nanomaterials: carbon nanofibers (CNFs), graphene oxide (GO),

73 gold nanoparticles (AuNPs). Similar studies have been done before with conventional

74 screen-printed electrodes [24-25]. It was expected that these modifications would

75 improve the sensitivity of the electrochemical detection of the analytes, as compared to

76 unmodified paper electrodes, obtaining a more conductive working electrode with

77 advantages for the development of low cost sensors. In order to apply electrochemical

78 treatments or in-situ synthesis of nanomaterials, the ink side of the paper substrate was

79 placed on top of the working electrode of a commercial screen-printed card, with the ink

80 acting as contact layer. The nanomaterials were added (or generated) on the uncoated

81 side, keeping the screen-printed electrode below unmodified and ready to study another

82 specimen. The modification with gold nanoparticles was carried out in-situ, and

83 monitored by chronopotentiometry. The procedures developed here have been

84 customised for each type of the nanomaterial. A multivariate optimization was used,

85 because this is the only approach that allows us to identify interactions among factors

86 [26-28]. Dopamine (a neurotransmitter that plays an important work in human life [29-

87 30]) was chosen as electrochemical probe. The analysis of the multivariant data

88 collected allowed us to identify the interaction of every factor with the response (current

89 intensity) and the interactions among them, by using the minimal number of

90 experiments. This approach reduces reagent consumption and working time. In this

91 case, we have used a full factorial design with a central point for the modification

92 involving graphene-oxide reduction or gold deposition. Impedance measurements were

93 also made to evaluate the resistance of the system with the paper electrode and how the

94 modification with nanomaterials can change it. The discussion is based on the results

95 obtained with the best conditions found for every modification procedure.

96 **2.   Experimental section**

97

98 **2.1. Materials and electrochemical instrumentation**

99 Screen-printed electrode cards were obtained from DropSens S.L. (SPCEs, ref.

100 DRP-110, Spain). Their working and an auxiliary electrode are made of carbon ink, and

101 the pseudoreference electrode is made of silver. A DSC connector (ref. DRP-DSC) from

102 the same company was used to connect them with the potentiostat.

103 Graphene oxides (GOs) were a gift from Instituto Nacional del Carbón (INCAR,

104 CSIC, Spain). They were made by pyrolysis of anthracene tars in a process to obtain

105 "coke", (fuel made of calcified coal). Graphite was obtained following a heat treatment

106 at 2800ºC. It was converted into GO by the modified Hummers' method [31].

107 Nanofibers were obtained from Grupo Antolin (Spain). Carbon paste (ref. C10903P14)

108 was acquired by Gwent group (United Kingdom).

109 The cellulose substrate was Whatman Grade 1 chromatography paper.

110 Hydrophobic wax patterns were printed on the paper by using a wax printer (Xerox

111 Colorqube 8570). A thermostat model (Nabertherm d-2804) was used to melt the wax

112 printed on paper Whatman Grade 1. The spray adhesive 3M Spray Mount^{TM} was

113 adquired by local stores.

114 Electrochemical measurements were carried out with a potentiostat (Autolab,

115 PGSTAT 10) controlled by the Autolab GPES software.

116 Impedance measurements were carried out with a potentiostat (Autolab

117 PGSTAT 12) controlled by the Autolab FRA software measuring a range from 1000 Hz

118 to 1 Hz (n=30).

119 **2.2. Reagents and preparation of solutions**

120 General reagents, Potassium hexacyanoferrate (II) trihydrate potassium

121 hexacyanoferrate (III), Tris (hydroxymethyl)aminomethane (Tris) and dopamine were

122 purchased from Sigma-Aldrich (USA). Water used was obtained from a Millipore Milli-

123 Q purification system (Millipore Direct-Q^{TM} 5). Solutions of sulphuric acid, sodium

124 hydroxide and phosphate buffer saline (PBS pH = 7) were prepared as supporting

125 electrolytes for the reduction of the graphene oxide and the rest of electrochemical

126 measurements. The solutions of dopamine were made in 0.1 M H_2SO_4.

127 Solutions of hexacyanoferrate (II/III) 0.01 M were prepared in a 0.1 M Tris-

128 HNO_3 pH = 7 buffer.

129 Paper patterns were fabricated on Whatman Grade 1 paper and then placed in a

130 thermostat at 90 ºC to melt the wax. The design was made by means of Inkscape

131 program.

132 The carbon ink used to modify the paper was made by the dissolution of the

133 commercial carbon paste in anhydrous N, N-dimethylformamide (DMF) in an

134 ultrasound bath for one hour. The concentration of the carbon paste was 20 % (w/w).

135 After cooling at room temperature, the paper was modified by addition of 2 µL of

136 carbon ink solution by drop casting on one of the sides, and was left to dry having a side

137 covered by ink (bottom side) and a side which will be used to add the nanomaterials and

138 samples to measure (upper side). This prepared cellulosic electrode was cut with an area

139 which covered the working electrode from the screen-printed platform and the ceramic

140 surface between the working and auxiliary electrode. The surface of the paper electrode

141 overlaying the working screen-printed card was covered by a protector and the rest was

142 covered by an adhesive spray. The final electrode was placed on the surface of the

143 working electrode of a screen-printed electrode card (SPCE). With this procedure there

144 was good contact between the carbon ink on the paper and the carbon ink on the SPCE

145 without any interference from the adhesive spray. Before the measurements, it was

146 verified that there was full overlap, and the solution added on the surface of the paper

147 electrode was not in contact with the working SPCE. In order to check that, we have

148 used the SPCE after a run with overlapping nanomaterials modified paper prepared by

149 the techniques described below. We have found that there were not differences with a

150 fresh SPCE, confirming therefore, that the solutions do not contact the underlying

151 SPCE.

152

153 **2.3. Modification of the prepared cellulose based electrodes**

154   Paper electrodes with carbon ink were modified with different types of

155 nanomaterials of different chemical nature: metallic (AuNPs) and carbon materials

156 (CNFs and GO) were employed. Two-dimensional (graphene) as well as one

157 (nanofibers) or zero (nanoparticles)-dimensional materials were considered, together

158 with hybrid modification procedures.

159

7

160   2.3.1. Modification with carbon nanofibers (CNFs)

161   Suspensions of CNFs were prepared in DMF and ultrapure water by solving

162   CNFs weighted in these solvents and put them in an ultrasonic bath for 1 hour. An

163   aliquot with volume varying from 1 to 4 µL and nanofiber concentration ranging from

164   0.1 to 10 mg/mL was deposited onto the upper part of the paper before placing it on the

165   screen-printed electrode card. Modified papers were kept at 80 ºC for 40 min when

166   working with DMF suspensions, whereas those modified with ultrapure water were left

167   to dry at room temperature.

168   2.3.2. Modification with graphene oxide (GO)

169   GO needs to be reduced in order to destroy oxide and hydroxide groups which

170   can interfere with the electrochemical signal. Two procedures for modification with GO

171   were carried out. The first one started with the preparation of suspensions of GO in

172   water, with different concentrations (1-100 mg/mL), and direct deposition of 6 µL on

173   the paper substrates, similarly to the procedure for modification with CNFs, previously

174   described. After the overlaying with the screen-printed electrode, the graphene oxide on

175   the paper-based working electrode (PWE) was reduced applying a constant current to

176   reduce the chemical groups of GO. The modification was followed by

177   chronopotentiometry. This reduction step was carried out in 3 different solvents (H_2SO_4,

178   NaOH, PBS 0.1 M). This process could be influenced by several factors interacting

179   among them, and therefore it was optimized for every solvent with a full factorial

180   design with a central point as is commented in. The most significant factors were

181   chosen for the factorial design (i.e. GO concentration, current intensity and time). The

182   upper and lower limits chosen were: 1 - 100 mg/L for GO concentration, -1 and -100

183   µA for current intensity, and 60 and 900 s for time. The full factorial design involved a

184   total of 19 experiments (duplicates of 8 different conditions and a triplicate of the

185   central point).

186

187   A second procedure for modification of paper electrodes with GO was tested

188   trying to simplify the protocol. In this case, 40 µL of GO solution (500 µg/mL on 0.1 M

189   NaCl) were placed on the upper side of the cellulose disc overlaying the surface of a

190   screen-printed working electrode. GO could be reduced applying either,

191   chronopotentiometry with different reduction intensities, or multicyclic voltammetry. In

192   the multicyclic voltammetry procedure, a potential from 0 V to – 1.5 V was applied at a

193   scan rate of 100 mV/s. The electrode was then ready for the electrochemical

194   measurements.

195   2.3.3. Modification with gold nanoparticles (AuNPs)

196   AuNPs were electrogenerated by chronopotentiometry after deposition of 40 µL

197   of a $HAuCl_4$ solution with different concentrations (0.1, 1 mM) on a cellulose paper

198   overlaying the surface of a screen-printed working electrode following a procedure

199   previously developed for screen-printed carbon electrodes in our research group [32].

200   2.3.4. Modification with hybrid nanostructures

201   All these nanomaterials (CNFs, GO and AuNPs) could be combined on the same

202   paper specimen generating a more conductive material, which could give a better

203   electrochemical signal than the paper modified with a single nanomaterial. Several

204   combinations were studied but preliminary results indicated that the most advantageous

205   involved the combination of a carbon nanomaterial (CNFs or reduced GO) with gold

206   nanoparticles. The electrodeposition of AuNPs on a paper modified with nanofibers was

207   also optimised by a factorial design whereas for the AuNPs/GO modification the best

9

208 individual conditions were employed. The limit values for the most significant factors

209 were: 0.1 and 1 mM for $AuCl_4^-$ concentration, -1 and -100 µA for current intensity and

210 60 and 180 s for time. The combination of several nanoparticles was also studied.

211 The Figure 1 summarizes the main routes used in this work for the preparation

212 of nanostructured paper electrodes.

213 **Insert figure 1**

214 **2.4. Analytical procedure**

215 The modified electrodes were evaluated by cyclic voltammetry (from 0 V to

216 +0.5 V at a scan rate of 50 mV/s), adding 40-µL drops of 100 µM dopamine solutions

217 (in 0.1 M H_2SO_4). The paper disc placed on the commercial screen-printed carbon

218 electrode was washed with ultrapure water (Milli-Q) between the modification and the

219 analysis step. The analytical signal monitored was the intensity of the peak current.

220 Results were obtained when the signal was stabilized.

221 **2.5. Paper substrate characterization**

222 The modified papers with the best properties were characterized by several

223 techniques such as Scanning Electron Microscopy (SEM) or Attenuated Total

224 Reflection (ATR) Spectrometry. SEM characterization was carried out at a microscope

225 JEOL 6610LV using 5-20 kV as voltage for the electron beam. The homogeneity of the

226 surface nanostructured with AuNPs was checked by scanning at different points of the

227 paper and recording the Electron Dispersive X-Ray (EDX) spectra with an EDX

228 attachment (JSM-6610). For obtaining lateral images of SEM papers, they were cut with

229 a scalpel, to obtain a clean cut. AuNPs were imaged by backscattered electron images.

230 The ATR measurements were carried out at both sides of the modified papers (also for

231 the GO reduced papers). A FTIR spectrometer (Varian Golden Gate, Varian 670-IR)

10

232   was used. The paper electrodes were placed on the surface of a diamond crystal to

233   monitor the ATR spectrum.

234   **3. Results and discussion**

235

236   **3.1. Preliminary studies on single-nanomaterial modification procedures**

237   The deposition of each nanomaterial generated electrodes with different

238   electrochemical behaviour. Figure 2A shows the morphology of the plain cellulose

239   network and cross sections of the substrates coated with the carbon ink. The paper used

240   had a thickness of around 150 μm. A 4 - 10 μm thick carbon layer could be observed at

241   the cross section of the paper. Ink deposition could also be monitored at the ATR

242   spectrum at Figure S1. As expected, the bare paper has the same spectrum at both sides,

243   showing peaks at 3340 nm associated to -OH groups and at 2906 nm due to -C-OH

244   bonds. CH_2OH groups were also identified at other studies with coated filter paper [33].

245   In contrast, the carbon ink that was employed as a contact layer with the working

246   electrode of the SPCE (from now, bottom side of the paper) showed only a huge band of

247   absorption associated to the carbon groups related to the ink. This agrees with the cross

248   sections observed at the SEM images in Figure 2A having ink only at one side of the

249   paper electrode.

250   INSERT FIGURE 2

251

252

253   3.1.1. Modification with CNFs

254   Modification with CNFs was carried out by drop casting an aliquot on the paper

255   substrates, and therefore the process was simple and not time consuming only needing

256   one cycle of cyclic voltammetry to get a stable signal. Several concentrations between

257 0.1 mg/mL and 1 mg/mL were studied with both working solvents (DMF and H_2O),

258 being DMF the best option to increase the intensity of the dopamine oxidation peak.

259 Increasing the added volume of the CNF solution on the paper did not improve the

260 signal of dopamine, and therefore, we have chosen for further studies the minimum

261 addition (2 μL of a stock solution of 1 mg/mL). The overall effect of the modification

262 was only a slight increase in the intensity current peaks. Results obtained showed an

263 increment of the oxidation peak current for dopamine around 0.31 and 0.57 μA using

264 carbon nanofibers suspended in H_2O and DMF. Reproducibility of the process was

265 better, as compared with the results with unmodified paper. Peak separation improves

266 considerably, indicating higher electronic transfer rates with a decrease in the ΔE_p

267 around 150 mV in comparison with unmodified paper electrodes.

268   The characterization of some modified papers with nanofibers under the SEM

269 microscope showed a modified upper-side totally covered by a homogenous layer of

270 carbon nanofibers in comparison to an unmodified paper with carbon ink as we can see

271 in Figure 2B. This would yield to higher conductive area in contact with the solution,

272 explaining the improvement of the oxidation peak current. However, the

273 homogenization of the CNFs through the paper thickness was not fully successful, since

274 the lateral view shows a layer of CNFs at the surface which was not observed in the

275 inner layers of the paper. This is probably due to the high aspect ratio of CNFs.

276 Therefore, this procedure results on a partially modified paper with two conductive

277 layers at the outer surfaces but with a not visibly-modified core of cellulose fibers with

278 low conductivity, which might explain the slight improvement of the electrochemical

279 behaviour observed.

280

281   3.1.2. Modification with AuNPs

282   The modification with AuNPs was made by the electrodeposition of Au (0)

283   using 1 mM HAuCl$_4$ in 0.1 M HCl and applying a reduction intensity of 100 µA. Unlike

284   the procedure with CNF paper electrodes, this procedure needs a stabilisation time

285   (quiet time) of 6 min after the reduction process to obtain a stable background signal.

286   Although this procedure takes longer than the AuNPs electrogeneration at a SPCE [32],

287   it requires fewer reagents than batch synthesis, and therefore, there is less contamination

288   on the cellulose matrix. [34-36] In this case, the effect obtained was a high improvement

289   on the intensity peaks of dopamine showing an anodic intensity around 2.4 µA, and on

290   the reproducibility of the process, in comparison with the results obtained on

291   unmodified paper. Peak separation decreases considerably showing a ΔEp around 40

292   mV obtaining a reversible electrochemical process of dopamine, as it is shown in Table

293   S1.

294   The AuNPs-modified paper electrodes were characterized under the SEM

295   (Figure 3), using backscattered electrons images and energy dispersive X-Ray

296   spectrometry (EDX). Au was clearly identified at the points seen as particles at the

297   backscattered electron´s image. The microanalysis study could not be carried out at the

298   lateral paper section due to instrumental limitations.   INSERT FIGURE 3

299

300   3.1.3.   Modification with graphene oxide (GO)

301   In order to prepare the nanostructured electrochemical transducer, graphene-

302   oxide must be reduced. This could be made by chronoamperometry or cyclic

303   voltammetry. The result was a reduced graphene-oxide (rGO) with a minimum amount

304   of oxides-groups which could interfere with the conductivity of the system. In this

305   work, a stabilisation time of around 6 min after the reduction process was also required

306   to obtain a stable background signal similar to that of the AuNPs paper electrodes.

13

307   Factorial design was applied to elucidate the most significant variables for

308   transducer preparation on different reduction solvents such as 0.1 M H_2SO_4, 0.1 M

309   NaOH and 0.1 M PBS (pH 7.0) by using chronopotentiometry. The variables studied

310   were the intensity of the current required for the reduction of GO, the time of

311   application and the concentration of GO, with the minimum and maximum values

312   shown previously chosen. The objective was to maximize the intensity of the current of

313   the anodic peak of dopamine, and to achieve the lowest ΔEp, in order to improve the

314   performance of the sensors developed with these transducers. Every variable made a

315   different influence on the response depending on the solvent. When H_2SO_4 was used as

316   electrolyte, the GO concentration and its interaction with the reduction current intensity

317   were the most important factors if we aimed the lowest ΔEp. However, long time was

318   necessary for obtaining the highest anodic peak current intensity, combined with the GO

319   concentration. GO reduction using PBS was found to be greatly influenced by the time

320   applied, having the intensity of the current applied a weaker effect. Finally, in case of

321   NaOH, no statistically significant factors were found. The Pareto charts and 3D plots

322   obtained by multifactorial design were used to identify the most significative variables

323   based on the optimization criteria: minimum ΔEp or maximum anodic peak current

324   intensity I_{pa} are in figures S4-S9. The best electrolyte for GO reduction at paper-ink

325   electrodes was NaOH. The results of the influence of every variable are shown in Table

326   S2 and S3. The optimum conditions were: 100 mg/L GO solution, employing a current

327   intensity of -100 µA for 60 s. Other possible options for reduction were 100 mg/L of

328   GO, with -100 µA for 60 s in H_2SO_4, or 100 ppm GO -10 µA for 900 s in PBS. All these

329   possibilities were better than the unmodified paper, with higher peak current intensities,

330   better reproducibility and a more reversible electrochemical process.

331   The second procedure for modification with graphene oxide and further

332   reduction also improves the electrochemical behaviour of dopamine obtaining current

333   intensity of 2.6 µA for the anodic peak and a ΔE_p of 44 mV. The reduction of graphene

334   oxide in this case involved 5 cycles of cyclic voltammetry. This was faster, because

335   there was no need to dry the solvent. Results are shown at Table S6.

336

337   We can conclude that the procedures used to deposit and reduce graphene oxide

338   generated the highest anodic intensity but also the highest background. This could

339   difficult the determination of analytes with lower concentration in comparison with the

340   modification with AuNPs. These procedures have better reproducibility compared with

341   the AuNPs modification. They could result in more precise and reliable transducers with

342   a simpler synthesis procedure than other methods described in the literature [37-38].

343

344   The modification of the paper electrodes with GO was studied under the SEM

345   but GO could not be identified neither at the paper disc or their cross sections. Although

346   this nanomaterial could potentially be seen at the SEM [39], in this case the cellulose

347   matrix of the electrode could have hindered its detection. ATR spectra did not change

348   after the modification with GO as we can see in Figure S2. It is possible that the

349   sensitivity of this technique was not good enough to characterize this type of

350   nanomaterial in a thick cellulose matrix.

351

352

353   **3.2. Nanostructuration with hybrid nanomaterials (CNFs or GO with AuNPs)**

15

354   Paper-based electrodes were modified by combinations of both carbon

355   nanomaterials and gold nanoparticles, yielding transducers with the best electrochemical

356   features. Results from both combinations were obtained after a quiet time of 6 min after

357   adding the drop on the paper electrode.

358   The CNFs modified paper electrodes had a higher conductive surface, and this

359   helped to improve the reproducibility of the electrodeposition of gold. A factorial design

360   was used to reduce the number of experiments and optimize the procedure. This

361   factorial design was made involving the following variables: current intensity, time of

362   application of the current intensity and $AuCl_4^-$ concentration. All the factors summarised

363   in Figure S3 were found significant ($p<0.05$) in response of obtaining high current

364   intensity peaks and an electrochemical process more reversible (lower ΔEp). Best

365   conditions were the highest concentration, the higher current intensity and the longest

366   reduction time (1 mM, -100 μA, 180 s) because of the higher anodic peak current

367   intensity and better reversibility obtained with a paper with CNFs + AuNPs with an

368   oxidation current intensity of 2 μA and a reversibility or ΔEp of 54 mV in comparison

369   with unmodified papers ($ip_a = 1.4$ μA, $\Delta Ep = 220$ mV) and papers modified with just

370   one type of these nanomaterials for dopamine oxidation. Table S7 show the results

371   obtained for the best hybrid combinations of nanomaterials studied. The results of the

372   influence of every variable are shown on Tables S4 and S5. Results obtained for higher

373   gold concentration or higher reduction current intensity did not show any improvement

374   on the response, and therefore they were discarded.

375   On the other hand, the GO-AuNPs hybrids were studied with the individual

376   optimal conditions (100 mg/L in NaOH by applying a reduction current intensity of 100

377   μA for 60 s, or reducing 40 μL of 500 mg/L of GO by applying 5 cycles at cyclic

378   voltammetry). The results obtained showed a higher improvement of the anodic process

16

379   and more reversible electrochemical behaviour, as compared with paper substrates

380   modified with only reduced GO. The anodic peak current intensity was the highest, and

381   the peak separation the lowest, but non-faradaic effects were very significant, with the

382   highest capacitive currents among of all the nanostructured possibilities explored

383   (Figure 4). Even though the two procedures of modification with graphene oxide have

384   similar results obtained with dopamine, the reduction by cyclic voltammetry results in

385   higher capacitive current, as compared with the other procedure shown in Figure 4. The

386   electrochemical process of dopamine by multicycle voltammetry in paper ink electrodes

387   with reduced graphene oxide appears at lower potential, as compared to the other case.

388   One possible hypothesis is the formation of AgCl over the reference electrode during

389   the reduction process due to the high concentration of Cl⁻.

390   The combination of the three types of nanomaterials did not make any improvement,

391   and therefore this option was not further explored.

392

393   **3.3. Comparison of the modified paper-based electrodes**

394   It has been shown that the modification of the paper electrodes with several

395   nanomaterials (CNFs, rGO, AuNPs) produced different electrochemical effects. Hybrids

396   of CNFs and AuNPs yielded the lowest capacitive current, whereas the rGO with

397   AuNPs hybrids produced the highest anodic peak intensity. Figure 4 summarizes the

398   most representative voltammograms.

399   Finally, in order to evaluate the improvement on sensitivity, the best electrodes

400   (rGO by NaOH with a reduction intensity current of 100 µA for 60 s with AuNPs and

401   CNFs with AuNPs) were tested by triplicate with increasing concentrations of dopamine

402   from 5 µM to 100 µM, and compared with those obtained with plain paper. Two

403   quantification techniques were used: square wave voltammetry (SWV, with 75 mV of

17

404 amplitude, 20 Hz of frequency, 2 mV of step potential, quiet time of 360 s) and

405 differential pulse voltammetry (DPV, with 20 mV of pulse amplitude, 2 mV of step

406 potential, quiet time of 360 s). The best linear regression and sensitivity was achieved

407 for the hybrid structure of CNFs (DMF) and AuNPs, by using DPV (ip_a (µA) = 0.0779

408 [Dopamine] (µM) - 0.049, R^2 = 0.989) with a LOD of 14 µM (n=6).

409 INSERT FIGURE 4

410 **3.4. Estimation of the resistance of paper-based electrodes by Electrochemical**
411 **Impedance Spectroscopy (EIS)**

412 Impedance measurements were carried out in order to evaluate this property at the

413 system under study and how it is affected by the modification with nanomaterials.

414 Measurements of impedance were made on SPCE with paper-based modified with the

415 best conditions. During a redox reaction at an electrode, the currents involved at the

416 capacitance of the double layer can be represented by the Randles-Ershler circuit. The

417 corresponding Nyquist diagram is shown in figure 5, in comparison with some Nyquist

418 diagram measured on paper based modified with carbon nanomaterials and gold

419 nanoparticles.

420 INSERT FIGURE 5

421 From this plot, we can calculate the charge transfer resistance Rt and the solution

422 resistance R_Ω. The latter in this case depends on the contact between SPCE and the

423 paper electrode. We have also carried out measurements of impedance on bare SPCE, to

424 calculate the resistance obtained on the paper electrode by substracting this value from

425 the total reading. Results are shown in table 1.

426 Resistance between the contact of the SPCE and the carbon ink on a non-nanostructured

427 paper was 146 Ω. This value decreases with the modification with AuNPs, and it is the

18

428   reason for the lower background at the voltammogram of dopamine (figure 4). In

429   contrast, reduced graphene oxide increases the resistance, in agreement with the higher

430   capacitive current shown at figure 4.

431   The charge transfer resistance (Rt) in turn had the lowest values for the

432   combinations of rGO-AuNPs and CNFs-AuNPs. This is probably due to the higher

433   conductivity of the system.

434   **Insert Table 1**

435   We have studied the variation of $E_{p/2}$ and E_p at different scan rates for these

436   nanomaterials electrode modifications. The representation of ($E_{p/2}$ - E_p) *vs.* scan rate

437   gave a bad linear regression coefficient. It could be considered that the processes are

438   reversible, since there was no influence of the scan rate. The representation of peak

439   intensity *vs.* $\nu^{1/2}$ was linear, indicating that the processes in our work were diffusion

440   controlled.

441   Regarding mass transfer processes, for reversible systems, surface concentration

442   of electroactive species depends only on the potential. Therefore, in our work, it can be

443   considered that peak currents are independent on the geometry of the electrode.

444   **4. Conclusions**

445   Paper working electrodes were modified by the deposition of several

446   nanomaterials in order to improve the conductivity of the transducer and obtaining a

447   better electrochemical signal. SEM-EDX and impedance measurements were

448   appropriate to characterize ink modified paper substrates unmodified and modified with

449   CNFs or AuNPs and observe the influence made by the nanomaterials added on the

450   resistance and conductivity parameters of the cellulose system. Optimization of the

451   transducers was carried out aiming the maximum anodic peak current for dopamine, and

19

ACCEPTED MANUSCRIPT

452 the minimum peak separation. The best transducers were those obtained with a

453 combination of carbon nanomaterials and gold nanoparticles: rGO-AuNPs and CNFs-

454 AuNPs. These nanomaterials increase the conductivity of the system improving

455 intensity currents and reversibility of the dopamine oxidation. Peak currents could be

456 considered independent of the geometry of the electrode. The LOD for dopamine

457 determination was 14 µM for CNF-AuNPs and 20 µM for rGO-AuNPs. These results

458 could be applied to other analytes. This work opens the path for the development of low

459 cost sensors with improved analytical characteristics through the use of metallic and/or

460 carbon nanostructures on paper substrates. As future perspectives, it is also possible to

461 develop a multiple layer portable sensor with the possibility to tune the modification of

462 the paper layers for a given purpose.

463

472

473

474 **5. References**

20

475 [1] S. K. Vashist, P. B. Luppa, L. Y. Yeo, A. Ozcan, J. H. T. Luong, Emerging

476 Technologies for Next-Generation Point-of-Care Testing, Trends in Biotechnology. 33

477 (2015) 692.

478 [2] J. Adkins, K. Boehle, C. Henry, Electrochemical Paper-based Microfluidics

479 Devices, Electrophoresis. 36 (2015) 1811.

480 [3] T. Rungsawang, P. Eakkasit, J. Adkins, C. Henry, O. Chailapakul, Development of

481 Electrochemical Paper-based Glucose Sensor using Cellulose-4-aminophenylboronic

482 acid-modified Screen-printed Carbon Electrode, Electroanalysis. 28 (2016) 462.

483 [4] P. Vijitvarasan, S. Oaew, W. Surareungchai, Paper-based Scanometric Assay for

484 Lead Ion Detection using DNAzyme, Analytica Chimica Acta. 896 (2015) 152.

485 [5] D. Zang, L. Ge, M. Yan, X. Song, J. Yu, Electrochemical Immunoassay on a 3D

486 Microfluidic Paper-based Device, Chem Commun. 48 (2012) 4683.

487 [6] J. Mettakoonpitak, K. Boehle, S. Nantaphol, P. Teengam, J. A. Adkins, M. Srisa-

488 Art, C. S. Henry, Electrochemistry on Paper-based Analytical Devices: A Review,

489 Electroanalysis. 28 (2016) 1420.

490 [7] N. Dossi, R. Toniolo, E. Piccin, S. Susmel, A. Pizzariello, G. Bontepelli, Pencil-

491 Drawn Dual Electrode Detectors to Discriminate Between Analytes Comigrating on

492 Paper-based Fluidic Devices but Undergoing Electrochemical Processes with Different

493 Reversibility, Electroanalysis. 25 (2013) 2515.

494 [8] W. Dungchai, O. Chailapakul, C. S. Henry, A Low-cost, Simple, and Rapid

495 Fabrication Method for Paper-based Microfluidics using Wax Screen-printing, Analyst.

496 136 (2011) 77.

497 [9] S. Wang, L. Ge, M. Yan, J Yu, X. Song, S. Ge, J. Huang, 3D Microfluidic Origami

498 Electrochemiluminescene Immunodevice for Sensitive Point-of-care Testing of

499 Carcinoma Antigen 125, Sensors and Actuators B. 176 (2013) 1.

500 [10] W. Li, L. Li, S. Li, X. Wang, M. Li, S. Wang, J. Yu, 3D Origami

501 Electrochemiluminiscence Immunodevice Based on Porous Silver-paper Electrode and

502 Nanoporous Silver Double-assisted Signal Amplification, Sensors and Actuators B. 188

503 (2013) 417.

504 [11] H. Wang, Y. Li, J. Wei, J. Xu, Y. Wang, G. Zheng, Paper-based Three-

505 Dimensional Microfluidic Device for Monitoring of Heavy Metals with a Camera Cell

506 Phone, Anal and Bioanal Chem. 406 (2014) 2799.

507 [12] G. P.M.K. Ciniciato, C. Lau, A. Cochrane, S. S. Sibbett, E. R. Gonzalez., P.

508 Atanassov, Development of Paper Base Electrodes: From Air-breathing to Paintable

509 Enzymatic Cathodes, Electrochim Acta. 82 (2012) 208.

510 [13] R. Liu, C. Zhang, M. Liu, Open Bipolar Electrode-electrochemiluminiscence

511 Imaging Sensing using Paper-based Microfluidics, Sensors and Actuators, B. 216

512 (2015) 255.

513 [14] M. Hasanzadeh, N. Shadjou, Electrochemical and Photoelectrochemical Nano-

514 immunesensing using Origami Paper Based Method, Materials Science & Engineering,

515 C. 61 (2016) 979.

516 [15] C. Fischer, A. Fraiwan, S. Choi, A 3D Paper-based Enzymatic Fuel Cell for Self-

517 powered. Low-cost Glucose Monitoring, Biosensors & Bioelectronics. 79 (2016) 193.

518 [16] M.M. Hamedi, A. Ainla, F. Guder, D.C. Christodouleas, M.T. Fernández-Abedul,

519 G.M. Whitesides, INTEGRATING ELECTRONICS AND MICROFLUIDICS ON

520 PAPER, Adv. Mat. 28 (25) (2016) 5054.

521 [17] A.C. Glavan, D. Christodouleas, B. Mosadegh, H.D. Yu, B. Smith, J. Lessing,

522 M.T. Fernández-Abedul, G.M. Whitesides, "Folding analytical devices for

523 electrochemical elisa in hydrophobic R^H paper", Anal. Chem. 86 (2014) 11999.

524 [18] E. Nuñez-Bajo, M.C. Blanco-Lopez, A. Costa-Garcia, M. T. Fernández-Abedul,

525 Integration of Gold-sputtered Electrofluidic Paper on Wire-included Analytical

526 Platforms for Glucose Biosensing, Biosensors & bioelectronics. 91 (2017) 824.

527 [19] B. Guntupalli, P. Liang, J-H. Lee, Y. Yang, H. Yu, J. Canoura, J. He, W. Li, Y.

528 Weizmann. Y. Xiao, Ambient Filtration Method to Rapidly Prepare Highly Conductive,

529 Paper-Based Porous Gold Films for Electrochemical Biosensing, ACS Appl. Mater.

530 Interfaces. 7 (2015) 27049.

531 [20] T.H. Costa, E. Song, R. P. Tortorich, J.W. Choi, A Paper-Based Electrochemical

532 Sensor Using Inkjet-Printed Carbon Nanotube Electrodes, ECS Journal of Solid State

533 Science and Technology. 4 (2015) S3044.

534 [21] A. Maattanen, U. Vanamo, P. Pulkkinen, T. Petri, B. Heikki, P. Johan, J. Peltonen,

535 A Low-cost Paper-based Inkjet-printed Platform for Electrochemical Analyses, Sensors

536 and Actuators, B. 177 (2013) 153.

537 [22] O. Amor-Gutiérrez, E. C. Rama, A. Costa-García, M.T. Fernández-Abedul, Paper-

538 based Maskless Enzymatic Sensor for Glucose Determination Combining Ink and Wire

539 Electrodes, Biosensors and Bioelectronics. 93 (2017) 40.

540 [23] E. Nuñez-Bajo, M.B. González-García, A. Costa-García, M.T. Fernández-Abedul,

541 Electrogeneration of Gold Nanoparticles on Porous-Carbon Paper-Based Electrodes and

542 Its Application for Inorganic Arsenic Determination in White Wines by

543 Chronoamperometric Stripping, Anal Chim. 2017 in press. DOI

544 10.1021/acs.analchem.7b00144.

545 [24] E.C. Rama, M.B. González-García, A. Costa-García, Competitive electrochemical

546 Immunosensor for amyloid-beta 1-42 Detection Based on Gold Nanostructured Screen-

547 Printed Carbon Electrodes, Sensors and Actuators B. 201 (2014) 567.

548 [25] M. M. Pereira da Silva Neves, M. B. G. García, C. Delerue-Matos, A. C. García,

549 Nanohybrid Materials as Transducer Surfaces for Electrochemical Sensing

550 Applications, Electroanalysis. 23 (2011) 63.

551 [26] M. A. Bezerra, R. E. Santelli, E. P. Oliveira, L.S. Villar, L. A. Escaleira, Response

552 Surface Methodology (RSM) as a Tool Optimization in Analytical Chemistry, Talanta.

553 76 (2998) 965.

554 [27] S. V. Kergaravat, M. I. Pividori, S. R. Hernández, Evaluation of Seven

555 Cosubstrates in the Quantification of Horseradish Peroxidase Enzyme by Square Wave

556 Voltammetry Talanta. 88 (2012) 468.

557 [28] C. R. T. Tarley, G. Silveira, W. N. Lopez dos Santos, G. D. Matos, E. G. Paranho

558 da Silva, M. A. Bezerra, M. Miró, S. L. C. Ferreira, Chemometric Tools in

559 Electroanalytical Chemistry: Methods for Optimization Based on Factorial Design and

560 Response Surface Methodology, Microchemical Journal. 92 (2009) 58.

561 [29] Q-M. Feng, M. Cai, C-G. Shi, N. Bao, H-Y. Gu, Integrated paper-based

562 electroanalytical devices for determination of dopamine extracted from striatum of rat,

563 Sensors and Actuators B. 209(2015) 870

24

564   [30] P. Rattanarat, D. Wijitar, S. Weena, C. Orawon, H. Charles, Sodium Dodecyl

565   sulfate-modified Electrochemical Paper-based Analytical Device for Determination of

566   Dopamine Levels in Biological Samples, Analytica chimica acta. 744 (2012) 1.

567   [31] A. S. Calvo, C. Botas, D. Martín-Yerga, P. Álvarez. JR. Menéndez, A. Costa-

568   García, Comparative Study of Screen-Printed Electrodes Modified with Graphene

569   Oxides Reduced by a Constant Current, J. Electrochem. Soc. 162 (2015) B282.

570   [32] G. Martinez-Paredes, M. B. González-García, A. Costa-García, In situ

571   Electrochemical Generation of Gold Nanostructured Screen-printed Carbon Electrodes.

572   Application to the Detection of Lead Underpotential Deposition, Electrochim Acta. 54

573   (2009) 4801.

574   [33] A.M. Youseff, S. Kamel, M.El-Sakhawy, M.A. El Samahy, Structural and

575   Electrical Properties of Paper-polyaniline Composite. Carbohydrate polymers 90 (2012)

576   1003.

577   [34] C. Villena, M. Bravo, B. Alonso, C. M. Casado, J. Losada, M. P. G. Armada, Size-

578   controlled Gold Nanoparticles Obtained from Electrodeposited Amidoferrocenylpoly

579   (propleneimine) Dendrimer-templates for the Electrochemical Sensing of Dopamine,

580   Applied Surface Science 420 (2017) 651.

581   [35] W. Cui, X. Fang, H. Zhao, Z. Li, H. Ren, An Electrochemical Sensor for Dopamine

582   based on Polydopamine Modified Reduced Graphene Oxide Anchored with Tin

583   Dioxide and Gold Nanoparticles, Anal. Methods 9 (2017) 5322.

584   [36] M. A. Alonso-Lomillo, O. Domínguez-Renedo, A. Saldaña-Botín, M. J. Arcos-

585   Martínez, Determination of Ascorbic Acid in Serum Samples by Screen-printed Carbon

586   Electrodes Modified with Gold Nanoparticles, Talanta 174 (2017) 733.

587 [37] V. Mani, M. Govidasamy, S. Chen, R. Karthik, S. Huang, Determination of

588 Dopamine Using a Glassy Carbon Electrode Modified with a Graphene and Carbon

589 Nanotube Hybrid Decorated With Molybdenum Disulfide Flowers, Microchim Acta
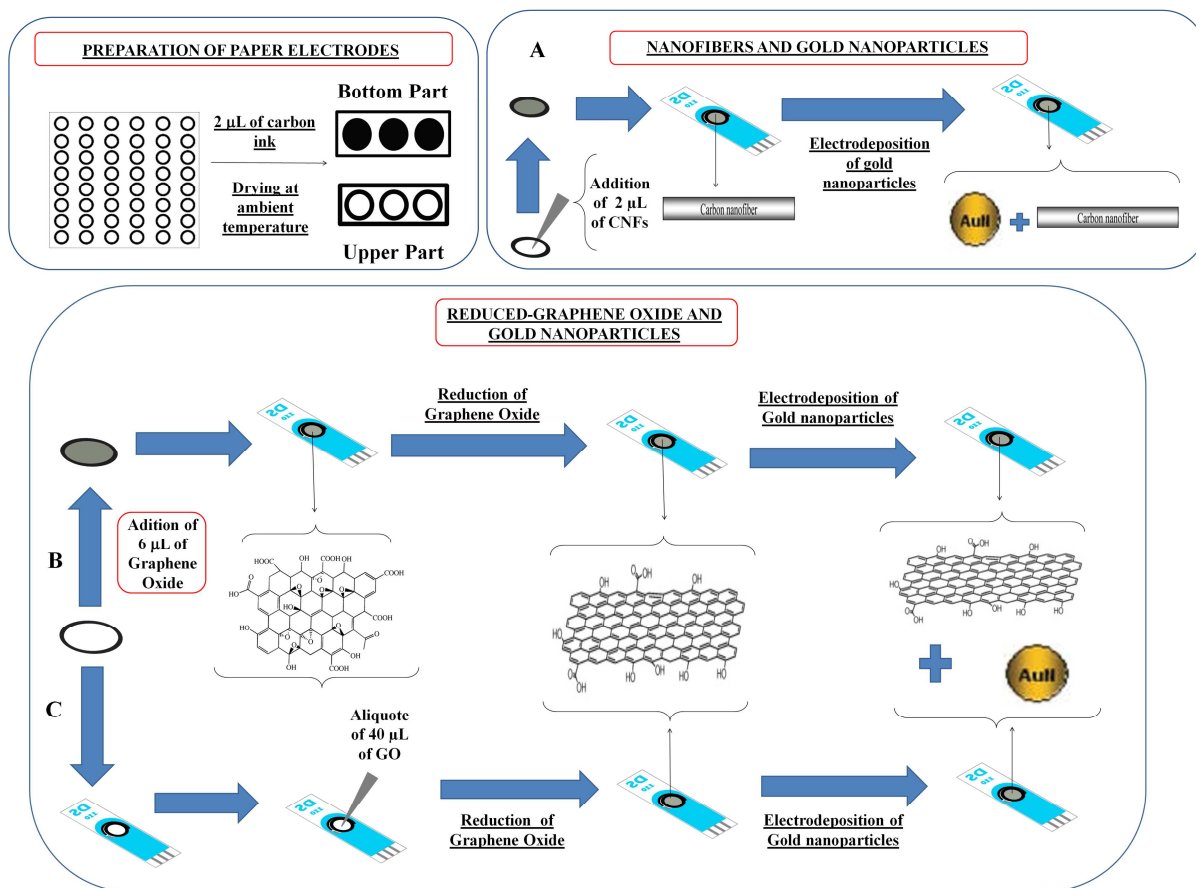
590 183 (2016) 2267.

591 [38] K. Huang, Q. Jing, Z. Wu, L. Wang, C.Wei, Enhanced sensing of Dopamine in the

592 Present of Ascorbic Acid Based on Graphene/poly(p-aminobenzoic acid) Composite

593 Film, Colloids and Surfaces B; Biointerfaces 88 (2011) 310.

594 [39] K. Grodecki, I. Jozwik, J.M. Baranowski, D. Teklinska, W. Strupinski SEM and

595 Raman Analysis of Graphene on SiC (0001), Micron. 80 (2016) 20.

596

Table 1. Charge transfer and surface resistance of hexacyanoferrate (II/III) 0.01 M corresponding to impedance measures at modified and unmodified paper electrodes. Values shown are the average of 3 measurements at independent electrodes.

| Transducer	Charge transfer resistance Rt (Ohm)	Surface resistance R_Ω (Ohm)	Resistance of the contact between carbon inks (Ohm)
Unmodified SPCE	184.9 ± 30	246 ± 57	
Unmodified paper	144 ± 3	392 ± 14	146
AuNPs	139 ± 10	328 ± 21	82
CNF	175.1 ± 50	409 ± 19	163
CNF+ AuNPs	99.8 ± 6	343 ± 74	97
rGO	99 ± 7	411 ± 42	165
rGO-AuNPs	84 ± 17	396 ± 53	150

Figure 1. Schematic diagram showing the preparation of the paper electrodes used in this work. (A) Modification of the upper part of the paper with both carbon nanofibers (CNFs) and electrodeposited AuNPs. (B) Modification of the upper side of paper with graphene-oxide (GO) before overlaying it on the screen-printed electrode card to electrodeposit AuNPs. (C) Modification of the upper part of paper with both GO and electrodeposited AuNPs
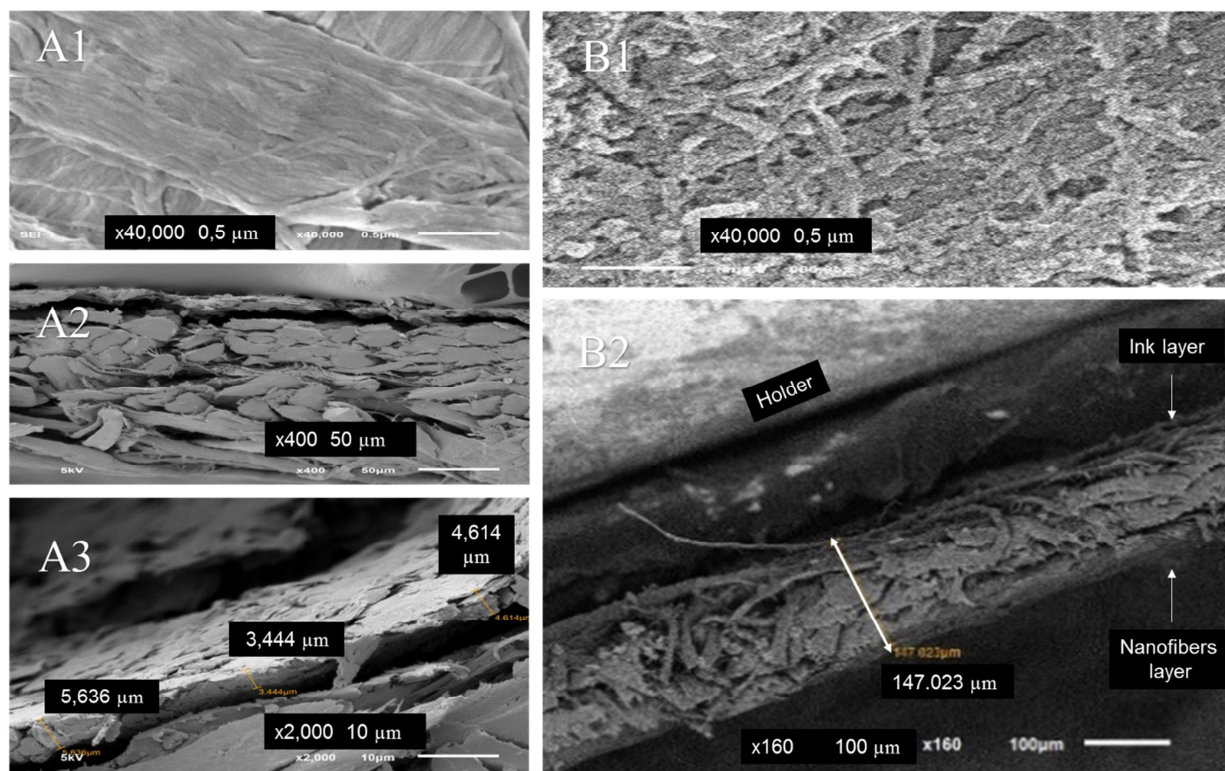
Figure (2). A) SEM micrographs of a paper disc with a carbon ink contact at one side. (A1) Morphology of the upper side (unmodified cellulose network). A2) and A3) Cross section with two different magnifications. (B) SEM images of a CNFs modified paper with carbon ink contact below. B1) Micrograph of the upper side. B2) Cross section.
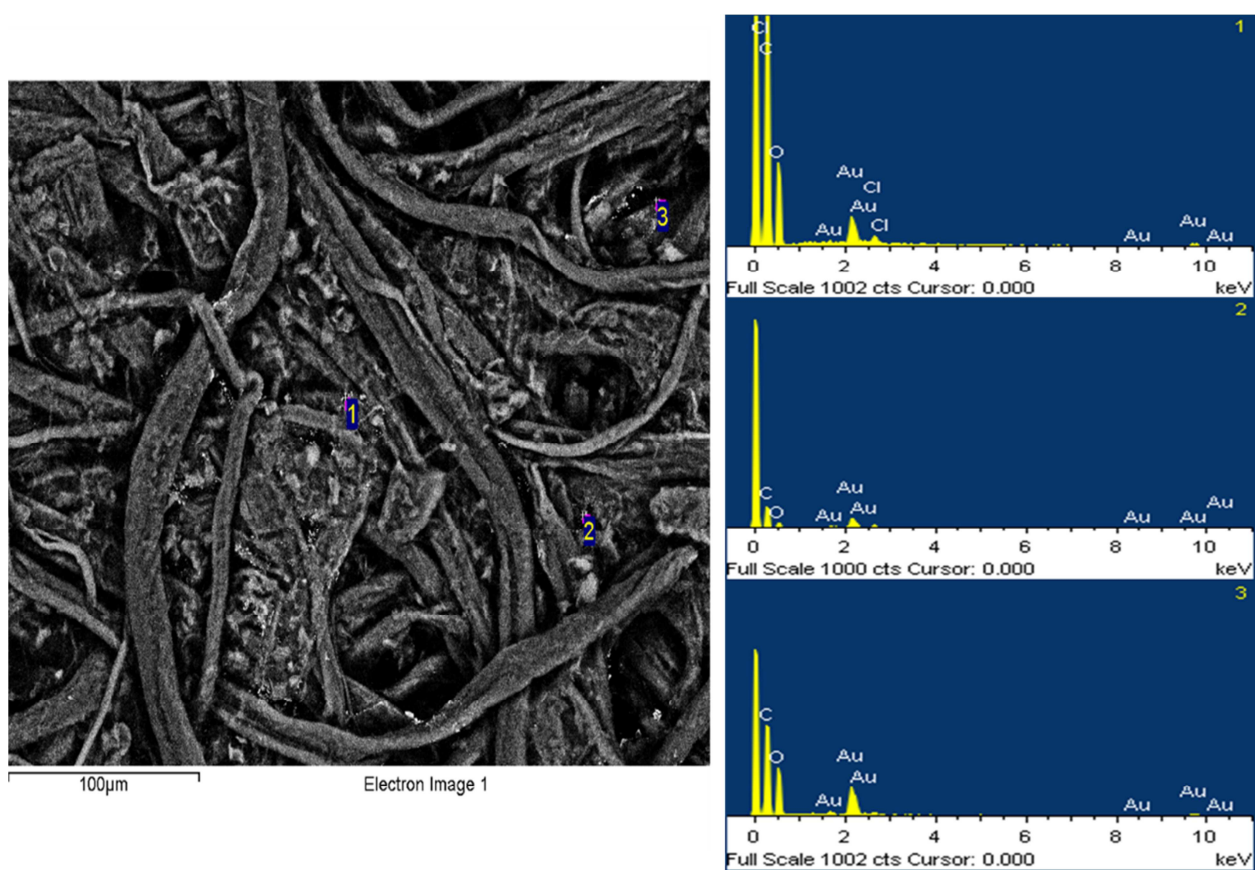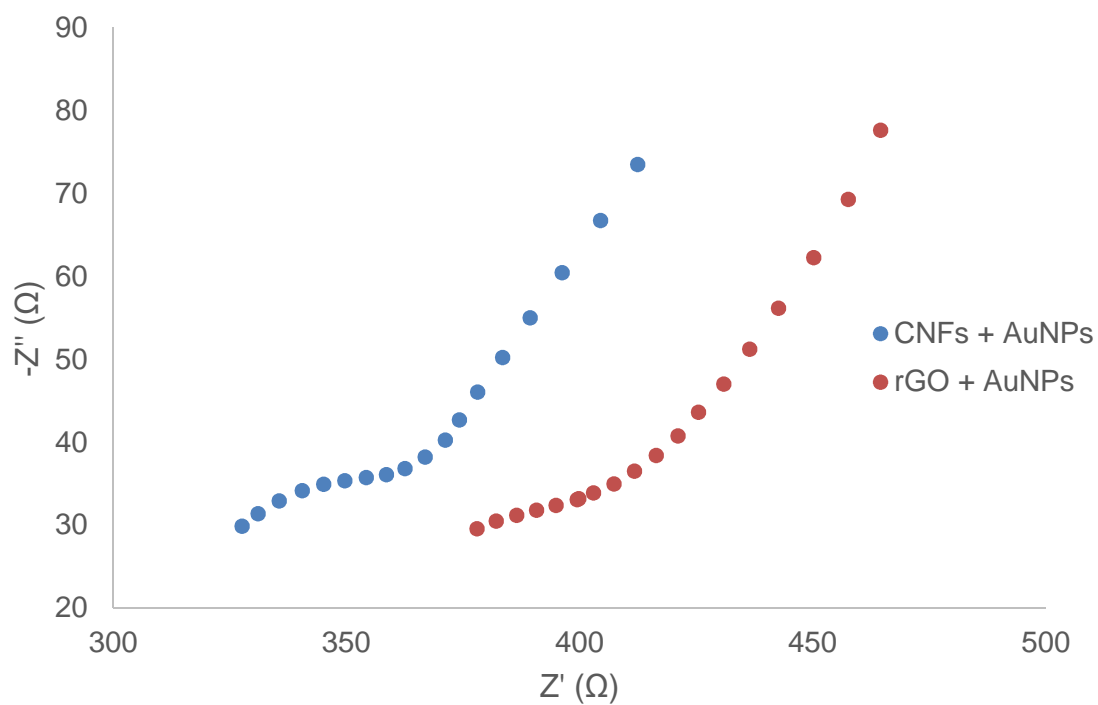
Figure (3). A) Backscattered electrons image of a AuNPs modified paper **B)** EDX spectra at 3 different points confirming the presence of gold and another paper impurities.
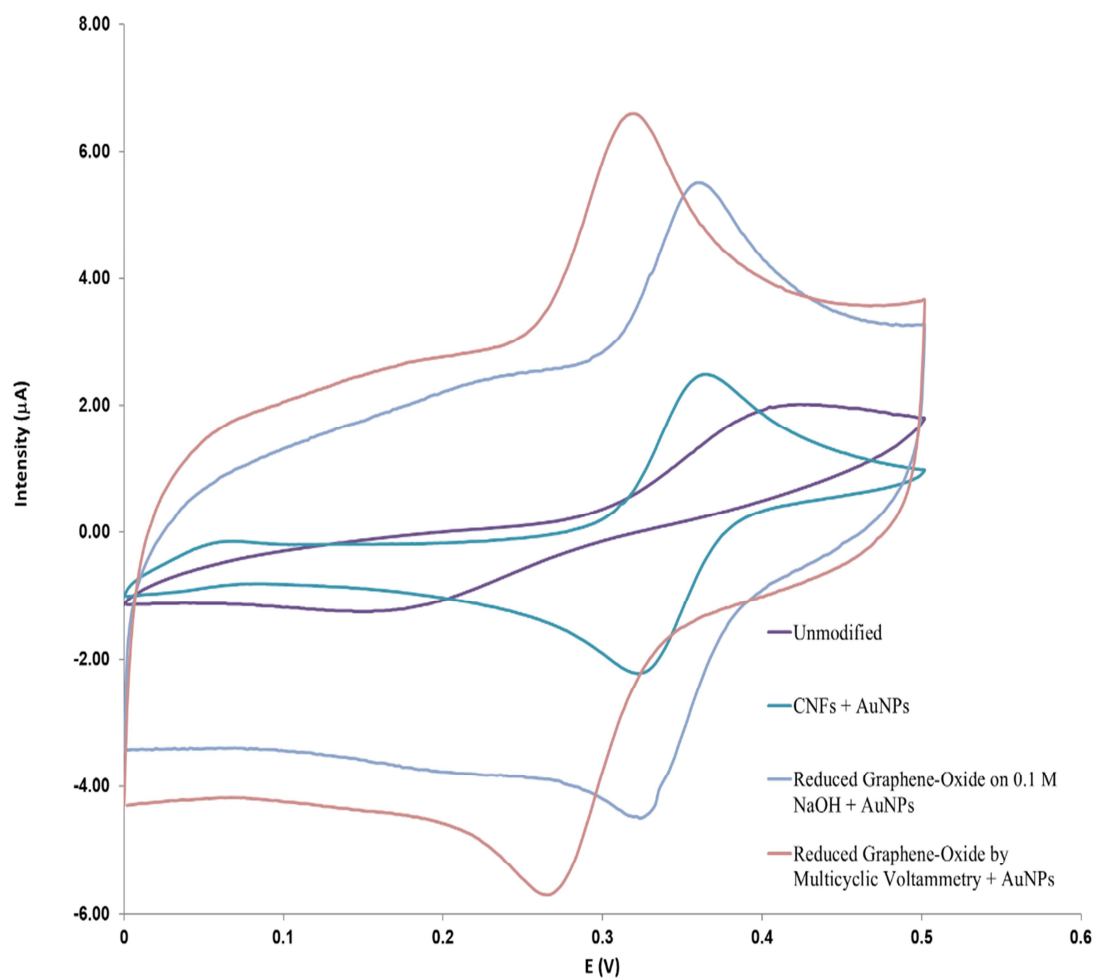
Figure 4: (A). Cyclic voltammetry of an unmodified paper electrode and several modified paper electrodes with different combinations of nanomaterials.

Figure 5: Nyquist diagram obtained in paper-based working electrodes modified with carbon nanomaterials and gold nanoparticles. The electrochemical probe was hexacyanoferrate (II/III) 0.01 M prepared in a 0.1 M Tris-HNO$_3$ pH = 7.0 buffer.